

CENTRAL SCHEMES FOR POROUS MEDIA FLOW

E. ABREU¹, F. FURTADO², F. PEREIRA¹ AND S. RIBEIRO¹

¹ State University of Rio de Janeiro, Nova Friburgo, RJ 28630-050, Brazil.

² University of Wyoming, Laramie, WY 82071-3036, U.S.A.

ABSTRACT

We are concerned with central differencing schemes for solving scalar hyperbolic conservation laws arising in the simulation of multiphase flows in heterogeneous porous media. We compare the Kurganov-Tadmor (KT) (Kurganov and Tadmor, 2000) semi-discrete central scheme with the Nessyahu-Tadmor (NT) (Nessyahu and Tadmor, 1990) central scheme. The KT scheme uses more precise information about the local speeds of propagation together with integration over nonuniform control volumes, which contain the Riemann fans. These methods can accurately resolve sharp fronts in the fluid saturations without introducing spurious oscillations or excessive numerical diffusion. Numerical simulations are presented for two-phase, two-dimensional flow problems in multi-scale heterogeneous petroleum reservoirs. We find the KT scheme to be considerably less diffusive, particularly in the presence of high permeability flow channels, which lead to strong restrictions on the time step selection; however, the KT scheme may produce incorrect boundary behavior.

1. INTRODUCTION

We are concerned with high resolution central schemes for solving scalar hyperbolic conservation laws arising in the simulation of multiphase flows in multidimensional heterogeneous petroleum reservoirs.

Many of the modern high resolution approximations for nonlinear conservation laws employ Godunov (Godunov, 1959) approach or the **REA** (reconstruct, evolve, average) algorithm, i.e., the approximate solution is represented by a piecewise polynomial which is **R**econstructed from the **E**volving cell **A**verages. The two main classes of Godunov methods are upwind and central schemes.

The Lax-Friedrichs (LxF) scheme (Lax, 1954) is the canonical first order central scheme, which is the forerunner of all central differencing schemes. It is based on piecewise constant approximate solutions. It also enjoys simplicity, i.e., it does not employ Riemann solvers and characteristic decomposition. Unfortunately the excessive numerical dissipation in the LxF recipe (of order $\mathcal{O}((\Delta X)^2/\Delta t)$) yields a poor resolution, which seems to have delayed the development of high resolution central schemes when compared with the earlier developments of the high resolution upwind methods. Only in 1990 a second order generalization to the LxF scheme was introduced by Nessyahu and Tadmor (NT) (Nessyahu and Tadmor, 1990). They used a staggered form of the LxF scheme and

replaced the first order piecewise constant solution with a van Leer's MUSCL-type piecewise linear second order approximation (Van Leer, 1979). The numerical dissipation in this new central scheme has an amplitude of order $\mathcal{O}((\Delta X)^4/\Delta t)$. When applying these methods to multiphase flow in highly heterogeneous petroleum reservoirs or aquifers we need to use decreasing time steps as the heterogeneity increases, yielding a greater numerical diffusion. To overcome this difficulty, Kurganov and Tadmor (KT) (Kurganov and Tadmor, 2000) combined ideas from the construction of the NT scheme with the Rusanov's method (Rusanov, 1961) to obtain the first second order central scheme that admits a semi-discrete formulation which is then coupled with an appropriate ODE solver. The resulting scheme has a much smaller numerical diffusion than the NT scheme. Due to the semi-discrete formulation, this numerical diffusion is independent of the time step used to evolve the ordinary differential equation. This property guarantees that no extra numerical diffusion will be added if the time step is enforced to decrease.

The main goal of this paper is to compare the KT semi-discrete central scheme with the NT central scheme for numerical simulations for two-phase, incompressible, two-dimensional flows in heterogeneous formations. These methods can accurately resolve sharp fronts in the fluid saturations without introducing spurious oscillations or excessive numerical diffusion. The NT scheme has recently been used in the numerical investigation of non-classical (transitional) waves in multidimensional three-phase (oil-gas-water) flows in petroleum reservoirs (see Abreu et al., 2004a,c,d,b).

Our numerical experiments indicate that the KT scheme is considerably less diffusive, particularly in the presence of viscous fingers, which lead to strong restrictions on the time step selection. On the other hand the KT scheme may produce incorrect boundary behavior in a typical two-dimensional geometry used in the study of porous media flows: the quarter of a five spot.

The results reported here indicate that a new multidimensional version of the KT scheme might be developed, aiming at a new scheme which inherits the low numerical diffusion of the KT approach, while showing correct boundary behavior for genuinely multidimensional problems.

Numerous methods have been introduced to solve two-phase flow problems in porous media. Among eulerian-lagrangian procedures we mention the Modified Method of Characteristics (Dahle et al., 1990, Douglas and Russell, 1982), the Modified Method of Characteristics with Adjusted Advection (Douglas et al., 1997), the Locally Conservative Eulerian Lagrangian Method (Douglas et al., 2000) and Eulerian Lagrangian Localized Adjoint Methods (Dahle et al., 1995). Additional techniques, to name just a few, include higher-order Godunov schemes (Bell et al., 1988), the front-tracking method (Glimm et al., 1983), the streamline upwind Petrov-Galerkin method (SUPG) (Coutinho et al., 1994, Coutinho and Parsons, 1999) and a second-order TVD-type finite volume scheme (Durlafsky, 1993) (this procedure aims at the modeling of flow through geometrically complex geological reservoirs). Each of these procedures has its advantages and disadvantages. We refer the reader to (Ewing and Wang, 2001, Douglas et al., 2000) and references cited there for a discussion of these methods.

We remark that central schemes are particularly interesting for the numerical simulation of multiphase flow problems in porous media because they have been formulated to solve

hyperbolic systems; this is not the case for several of the procedures mentioned above, which have been developed only for scalar equations.

This paper is organized as follows. In Section 2 we discuss our strategy for solving numerically the model for two-phase flows, immiscible and incompressible displacement in heterogeneous porous media introduced in Section 1. In Section 3 we will discuss the application of the central differencing schemes for porous media flow. In Section 4 we present the computational solutions for the model problem considered here and our conclusions.

2. NUMERICAL APPROXIMATION OF TWO-PHASE FLOW

We consider a model for two-phase flow, immiscible and incompressible displacement in heterogeneous porous media. The governing equations are highly nonlinear and lead to shock formation, and with or without diffusive terms they are of practical importance in petroleum engineering (Peaceman, 1977, Chavent and Jaffré, 1986). See also (Furtado and Pereira, 2003) and the references therein for recent studies for the scale-up problem for such equations.

The conventional theoretical description of two-phase (oil-water) flow in a porous medium, in the limit of vanishing capillary pressure, is via Darcy's law coupled to the Buckley-Leverett equation. The two phases will be referred to as water and oil, and indicated by the subscripts w and o , respectively. We also assume that the two fluid phases saturate the pores. With no sources or sinks, and neglecting the effects of gravity these equations are (see Peaceman, 1977):

$$\nabla \cdot \mathbf{v} = 0, \quad \mathbf{v} = -\lambda(s)K(\mathbf{x})\nabla p, \quad (1)$$

$$\frac{\partial s}{\partial t} + \nabla \cdot (f(s)\mathbf{v}) = 0. \quad (2)$$

Here, \mathbf{v} is the total seepage velocity, s is the water saturation, $K(\mathbf{x})$ is the absolute permeability, and p is the pressure. The constant porosity has been scaled out by a change of the time variable. The constitutive functions $\lambda(s)$ and $f(s)$ represent the total mobility and the fractional flow of water, respectively.

2.1. Operator splitting for two-phase flow. An operator splitting technique is employed for the computational solution of the saturation equation (2) and the pressure equation (1) in which they are solved sequentially with distinct time steps. This splitting scheme has proved to be computationally efficient in producing accurate numerical solutions for two-phase flow. We refer the reader to (Douglas et al., 1997) and references therein for more details on the operator splitting technique; see also (Abreu et al., 2004b,a,c,d) for applications of this strategy for three phase flows that take into account capillary pressure (diffusive effects).

Typically, for computational efficiency, larger time steps are used for the pressure calculation (Equation 1). The splitting allows time steps for the pressure-velocity calculation that are longer than those for the convection calculation. Thus, we introduce two time steps: Δt_c for the solution of the hyperbolic problem for the convection, and Δt_p for the pressure-velocity calculation so that $\Delta t_p \geq \Delta t_c$. We remark that in practice variable time steps are always useful, especially for the convection micro-steps subject dynamically to a *CFL* condition.

For the pressure solution (the pertinent elliptic equation), we use a (locally conservative) hybridized mixed finite element discretization equivalent to cell-centered finite differences (Furtado and Pereira, 2003, Douglas et al., 1997), which effectively treats the rapidly changing permeabilities that arise from stochastic geology and produces accurate velocity fields. The pressure and the Darcy velocity are approximated at times $t^m = m\Delta t_p$, $m = 0, 1, 2, \dots$. The linear system resulting from the discretized equations can be solved by a preconditioned conjugate gradient procedure (PCG) (see Douglas et al. (1997) and the references therein) or by a multi-grid procedure. The saturation equation is approximated at times $t_\kappa^m = t^m + \kappa\Delta t_c$ for $t^m < t_\kappa^m \leq t^{m+1}$ that take into account the advective transport of water. We remark that we must specify the water saturation at $t = 0$.

We use high resolution central differencing schemes (see Nessyahu and Tadmor, 1990, Kurganov and Tadmor, 2000) for solving the scalar hyperbolic conservation laws arising in the convection of the fluid phases in heterogeneous porous media for two-phase flows - we will discuss the application of these schemes for two-phase flows in section 4. These methods can accurately resolve sharp fronts in the fluid saturations without introducing spurious oscillations or excessive numerical diffusion.

3. CENTRAL DIFFERENCING SCHEMES FOR POROUS MEDIA FLOW

In this section, we shall discuss the application of the family of high resolution, non-oscillatory, conservative central differencing schemes, introduced by Nessyahu and Tadmor (NT) and Kurganov and Tadmor (KT) for the numerical approximation of the scalar hyperbolic conservation law modeling the convective transport of fluid phases in two-phase flows and their coupling with lowest order Raviart-Thomas (Raviart and Thomas, 1977) locally conservative mixed finite elements for the associated elliptic problem (Eq. (1)).

These central schemes enjoy the main advantage of Godunov-type central schemes: simplicity, i.e., they employ neither characteristic decomposition nor approximate Riemann solvers. This makes them universal methods that can be applied to a wide variety of physical problems, including hyperbolic systems. In the following sections 3.1 and 3.2 we will discuss the main ideas of the NT and KT central schemes coupled with the mixed finite element discretization mentioned above. We will not repeat here all the details involved in the development of the NT and KT schemes; instead, we refer the reader to Nessyahu and Tadmor (1990) and Kurganov and Tadmor (2000) for this material.

3.1. The Nessyahu-Tadmor central scheme for two-phase flows. Consider the following scalar hyperbolic conservation law,

$$\frac{\partial s}{\partial t} + \frac{\partial}{\partial x}(x_v f(s)) + \frac{\partial}{\partial y}(y_v f(s)) = 0, \quad (3)$$

where $x_v \equiv x_v(x, y, t)$ and $y_v \equiv y_v(x, y, t)$ denote the x and y components of the velocity field \mathbf{v} (see Eq. 1). The cell averages at time t_κ^m are

$$\bar{S}_{j,k}(t_\kappa^m) \equiv \frac{1}{\Delta X \Delta Y} \int_{x_{j-\frac{1}{2}}}^{x_{j+\frac{1}{2}}} \int_{y_{k-\frac{1}{2}}}^{y_{k+\frac{1}{2}}} s(x, y, t_\kappa^m) dx dy. \quad (4)$$

We first construct from equation (4) a piecewise linear approximation of the form

$$\begin{aligned} \tilde{S}_{j,k}(x, y, t_\kappa^m) &= \bar{S}_{j,k}(t_\kappa^m) + (x - x_j) \frac{1}{\Delta X} \dot{S}_{j,k}'(t_\kappa^m) + (y - y_k) \frac{1}{\Delta Y} \dot{S}_{j,k}''(t_\kappa^m), \\ x_{j-\frac{1}{2}} &\leq x \leq x_{j+\frac{1}{2}}, \quad y_{k-\frac{1}{2}} \leq y \leq y_{k+\frac{1}{2}}. \end{aligned} \quad (5)$$

In Eq. (5), the discrete slopes along the x and y directions satisfy

$$\frac{\dot{S}_{j,k}'(t_\kappa^m)}{\Delta X} = (S_x)_{j,k}(t_\kappa^m) + O(\Delta X) \quad \text{and} \quad \frac{\dot{S}_{j,k}''(t_\kappa^m)}{\Delta Y} = (S_y)_{j,k}(t_\kappa^m) + O(\Delta Y), \quad (6)$$

to guarantee second-order accuracy.

The reconstruction (4)-(5) retains conservation, i.e.:

$$\frac{1}{\Delta X \Delta Y} \int_{x_{j-\frac{1}{2}}}^{x_{j+\frac{1}{2}}} \int_{y_{k-\frac{1}{2}}}^{y_{k+\frac{1}{2}}} \tilde{S}(x, y, t_\kappa^m) dx dy = \bar{S}_{j,k}(t_\kappa^m). \quad (7)$$

The time evolution of this reconstruction is based on the integration of the conservation law (3) over staggered volumes $I_{j+\frac{1}{2},k+\frac{1}{2}} \times [t_\kappa^m, t_\kappa^m + \Delta t_c]$ (dashed grid in Figure 1). The piecewise bilinear approximation of the solution is evolved in time, and then the result is projected on the staggered cells (dashed grid) $I_{j+\frac{1}{2},k+\frac{1}{2}}$ (see Figure 1) to yield new cell averages denoted by

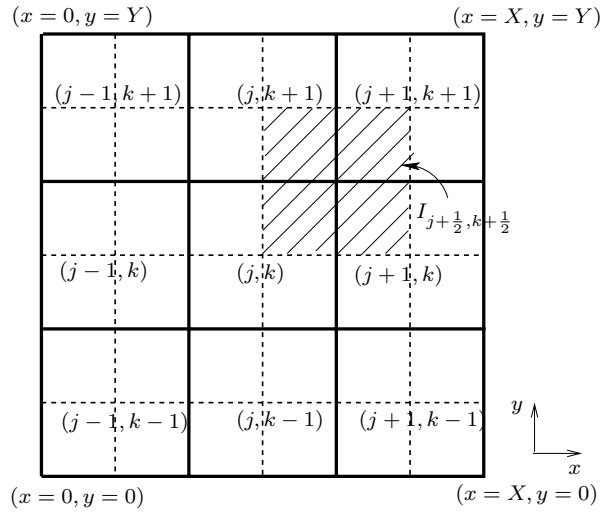


FIGURE 1. Evolution step at each time level t_κ^m , $t^m < t_\kappa^m \leq t^{m+1}$, for the two-dimensional NT central differencing scheme.

$$\begin{aligned} \bar{S}_{j+\frac{1}{2},k+\frac{1}{2}}(t_\kappa^m + \Delta t_c) &= \frac{1}{\Delta X \Delta Y} \int_{x_j}^{x_{j+1}} \int_{y_k}^{y_{k+1}} s(x, y, t_\kappa^m + \Delta t_c) dx dy, \\ x_j &\leq x \leq x_{j+1}, \quad y_k \leq y \leq y_{k+1}. \end{aligned} \quad (8)$$

These new staggered cell averages are obtained integrating the conservation law (3) following the same manipulations as described in Nessyahu and Tadmor (1990) (denote

$\alpha_x \equiv \frac{\Delta t_c}{\Delta X}$ and $\alpha_y \equiv \frac{\Delta t_c}{\Delta Y}$):

$$\begin{aligned}
\bar{S}_{j+\frac{1}{2},k+\frac{1}{2}}(t_\kappa^m + \Delta t_c) &= \frac{1}{4}(\bar{S}_{j,k}(t_\kappa^m) + \bar{S}_{j,k+1}(t_\kappa^m) + \bar{S}_{j+1,k}(t_\kappa^m) + \bar{S}_{j+1,k+1}(t_\kappa^m)) \\
&+ \frac{1}{16} \left[S'_{j,k}(t_\kappa^m) + S'_{j,k+1}(t_\kappa^m) - S'_{j+1,k}(t_\kappa^m) - S'_{j+1,k+1}(t_\kappa^m) \right. \\
&\quad \left. + \dot{S}_{j,k}(t_\kappa^m) - \dot{S}_{j,k+1}(t_\kappa^m) + \dot{S}_{j+1,k}(t_\kappa^m) - \dot{S}_{j+1,k+1}(t_\kappa^m) \right] \quad (9) \\
&+ \frac{\alpha_x}{2} \left[{}^x v_{j,k}(t_\kappa^m + \frac{\Delta t_c}{2}) f(S_{j,k}(t_\kappa^m + \frac{\Delta t_c}{2})) + {}^x v_{j,k+1}(t_\kappa^m + \frac{\Delta t_c}{2}) f(S_{j,k+1}(t_\kappa^m + \frac{\Delta t_c}{2})) \right. \\
&\quad \left. - {}^x v_{j+1,k}(t_\kappa^m + \frac{\Delta t_c}{2}) f(S_{j+1,k}(t_\kappa^m + \frac{\Delta t_c}{2})) - {}^x v_{j+1,k+1}(t_\kappa^m + \frac{\Delta t_c}{2}) f(S_{j+1,k+1}(t_\kappa^m + \frac{\Delta t_c}{2})) \right] \\
&+ \frac{\alpha_y}{2} \left[{}^y v_{j,k}(t_\kappa^m + \frac{\Delta t_c}{2}) f(S_{j,k}(t_\kappa^m + \frac{\Delta t_c}{2})) + {}^y v_{j+1,k}(t_\kappa^m + \frac{\Delta t_c}{2}) f(S_{j+1,k}(t_\kappa^m + \frac{\Delta t_c}{2})) \right. \\
&\quad \left. - {}^y v_{j,k+1}(t_\kappa^m + \frac{\Delta t_c}{2}) f(S_{j,k+1}(t_\kappa^m + \frac{\Delta t_c}{2})) - {}^y v_{j+1,k+1}(t_\kappa^m + \frac{\Delta t_c}{2}) f(S_{j+1,k+1}(t_\kappa^m + \frac{\Delta t_c}{2})) \right].
\end{aligned}$$

The fluxes in equation (9) are smooth at the vertices of the cell defining the integration volume, since these vertices are located at the centers of non-staggered cells (see Figure 1). The spatial integrals in both x and y directions are approximated by the second-order trapezoid quadrature rule and the temporal integrals are approximated by the midpoint quadrature rule under the restriction of a CFL-type constraint. The approximation of the fluxes in (9) make use of the midpoint values in time as a predictor step. So, by Taylor expansion and the conservation law (3) we can use

$$S_{j,k}(t_\kappa^m + \frac{\Delta t_c}{2}) = \bar{S}_{j,k}(t_\kappa^m) - \frac{\Delta t_c}{2} \left[{}^x v_{j,k}(t_\kappa^m) \frac{1}{\Delta X} f'_{j,k}(t_\kappa^m) + {}^y v_{j,k}(t_\kappa^m) \frac{1}{\Delta Y} \dot{f}_{j,k}(t_\kappa^m) \right] \quad (10)$$

to approximate the midpoint values $S_{j,k}(t_\kappa^m + \frac{\Delta t_c}{2})$ since these values are bounded away from the jump discontinuities along the edges. In Eq. (10),

$$\frac{f'_{j,k}(t_\kappa^m)}{\Delta X} = (f_x)_{j,k}(t_\kappa^m) + O(\Delta X) \quad \text{and} \quad \frac{\dot{f}_{j,k}(t_\kappa^m)}{\Delta Y} = (f_y)_{j,k}(t_\kappa^m) + O(\Delta Y) \quad (11)$$

are the numerical derivatives of the gridfunction $\{f_{j,k}\}$ in the x and y directions, respectively. The numerical derivatives (6) and (11) are chosen to produce a second order scheme for the approximation of (3) and to avoid spurious oscillations, it is essential to reconstruct these discrete derivatives with built-in nonlinear limiters. In this work we use

the following MinMod limiter

$$\begin{aligned} (S_x)_{j,k}(t_\kappa^m) &= \text{MM}\theta \frac{1}{\Delta x} \{ \bar{S}_{j-1,k}(t_\kappa^m), \bar{S}_{j,k}(t_\kappa^m), \bar{S}_{j+1,k}(t_\kappa^m) \} \\ &:= \text{MM} \left(\theta \frac{\Delta S_{j+1/2,k}(t_\kappa^m)}{\Delta x}, \frac{\Delta S_{j-1/2,k}(t_\kappa^m) - \Delta S_{j+1/2,k}(t_\kappa^m)}{2\Delta x}, \theta \frac{\Delta S_{j-1/2,k}(t_\kappa^m)}{\Delta x} \right); \end{aligned} \quad (12)$$

$$\begin{aligned} (f_x)_{j,k}(t_\kappa^m) &= \text{MM}\theta \frac{1}{\Delta x} \{ f_{j-1,k}(t_\kappa^m), f_{j,k}(t_\kappa^m), f_{j+1,k}(t_\kappa^m) \} \\ &:= \text{MM} \left(\theta \frac{\Delta f_{j+1/2,k}(t_\kappa^m)}{\Delta x}, \frac{\Delta f_{j-1/2,k}(t_\kappa^m) - \Delta f_{j+1/2,k}(t_\kappa^m)}{2\Delta x}, \theta \frac{\Delta f_{j-1/2,k}(t_\kappa^m)}{\Delta y} \right), \end{aligned} \quad (13)$$

where Δ is the centered difference, $\Delta S_{j+1/2,k}(t_\kappa^m) = \bar{S}_{j+1,k}(t_\kappa^m) - \bar{S}_{j,k}(t_\kappa^m)$. We refer the reader to Nessyahu and Tadmor (1990) and Kurganov and Tadmor (2000) and the references therein for the various options of the form of such discrete derivatives.

In our sequential scheme, when solving for the saturation in time, the total velocity \mathbf{v} is given by the solution of the velocity-pressure equation. Recall that the solution of Eq. (1) utilizes the lowest order Raviart-Thomas mixed finite element method. Thus, the computed total velocity \mathbf{v} is discontinuous at the vertices of the original non-staggered grid cells. This constitutes a difficulty for the staggered scheme (9), which requires the values of the total velocity \mathbf{v} at these vertices at every other time step. To avoid this difficulty we employ the non-staggered version of the NT scheme.

To turn the staggered scheme (9) into a non-staggered scheme, we re-average reconstructed values of the underlying staggered scheme, thus recovering the cell averages of the central scheme over the original non-staggered grid cells. First we reconstruct a piecewise bilinear interpolant at the time step $t = t_\kappa^m + \Delta t_c$

$$\begin{aligned} \tilde{S}_{j+\frac{1}{2},k+\frac{1}{2}}(x,y,t) &= \bar{S}_{j+\frac{1}{2},k+\frac{1}{2}}(t) + (x - x_{j+\frac{1}{2}}) \frac{1}{\Delta X} \dot{S}_{j+\frac{1}{2},k+\frac{1}{2}}(t) \\ &+ (y - y_{k+\frac{1}{2}}) \frac{1}{\Delta Y} \dot{S}_{j+\frac{1}{2},k+\frac{1}{2}}(t), \quad x_j \leq x \leq x_{j+1}, \quad y_k \leq y \leq y_{k+1}, \end{aligned} \quad (14)$$

as in (5), through the staggered cell averages given by (9), and re-averaged it over the original grid cells, giving the following non-staggered scheme also at $t = t_\kappa^m + \Delta t_c$:

$$\begin{aligned} \bar{S}_{j,k}(t) &= \frac{1}{4} (\bar{S}_{j-\frac{1}{2},k-\frac{1}{2}}(t) + \bar{S}_{j-\frac{1}{2},k+\frac{1}{2}}(t) + \bar{S}_{j+\frac{1}{2},k-\frac{1}{2}}(t) + \bar{S}_{j+\frac{1}{2},k+\frac{1}{2}}(t)) \\ &+ \frac{1}{16} (\dot{S}_{j-\frac{1}{2},k-\frac{1}{2}}(t) + \dot{S}_{j-\frac{1}{2},k+\frac{1}{2}}(t) - \dot{S}_{j+\frac{1}{2},k-\frac{1}{2}}(t) - \dot{S}_{j+\frac{1}{2},k+\frac{1}{2}}(t)) \\ &+ \frac{1}{16} (\dot{S}_{j-\frac{1}{2},k-\frac{1}{2}}(t) - \dot{S}_{j-\frac{1}{2},k+\frac{1}{2}}(t) + \dot{S}_{j+\frac{1}{2},k-\frac{1}{2}}(t) - \dot{S}_{j+\frac{1}{2},k+\frac{1}{2}}(t)). \end{aligned} \quad (15)$$

3.2. The Kurganov-Tadmor central scheme for two-phase flows. The first multi-dimensional extension of the KT scheme was presented in Kurganov and Tadmor (2000). This extension used the dimension by dimension approach, that is, the numerical fluxes computed along the x and y directions are viewed as a generalization of the one spatial dimension numerical fluxes. This approach consists of the following steps: at each time step t_κ^m and at each cell $I_{j,k}$,

- (i) we compute the difference of the numerical fluxes in one spatial dimension in the x direction while y remains constant and equals to y_k . Let's denote this difference by

$$F_{j+1/2,k}^x(t) := \frac{H_{j+1/2,k}^x(t) - H_{j-1/2,k}^x(t)}{\Delta X}.$$

We refer the reader to Kurganov and Tadmor (2000) for a detailed description.

- (ii) Analogously, we compute the difference of the numerical fluxes in one spatial dimension in the y direction while x remains constant and equals to x_j . This difference is denoted by

$$F_{j,k+1/2}^y(t) := \frac{H_{j,k+1/2}^y(t) - H_{j,k-1/2}^y(t)}{\Delta Y}.$$

- (iii) The cell average $\bar{S}_{j,k}(t_\kappa^m + \Delta t_c)$ in the next time step $t_\kappa^m + \Delta t_c$ is then the solution of the following differential equation

$$\begin{aligned} \frac{d}{dt} S_{j,k}(t) &= -(F_{j+1/2,k}^x(t) + F_{j,k+1/2}^y(t)) \\ &= -\frac{H_{j+1/2,k}^x(t) - H_{j-1/2,k}^x(t)}{\Delta X} - \frac{H_{j,k+1/2}^y(t) - H_{j,k-1/2}^y(t)}{\Delta Y}, \end{aligned} \quad (16)$$

where the numerical fluxes $H_{j+1/2,k}^x(t)$ and $H_{j,k+1/2}^y(t)$ are

$$\begin{aligned} H_{j+1/2,k}^x(t) &:= \frac{1}{2} \left[x_{v_{j+1/2,k}}(t) \cdot f(S_{j+1/2,k}^+(t)) + x_{v_{j+1/2,k}}(t) \cdot f(S_{j+1/2,k}^-(t)) \right] \\ &\quad - \frac{a_{j+1/2,k}^x(t)}{2} \left[S_{j+1/2,k}^+(t) - S_{j+1/2,k}^-(t) \right]; \end{aligned} \quad (17a)$$

$$\begin{aligned} H_{j,k+1/2}^y(t) &:= \frac{1}{2} \left[y_{v_{j,k+1/2}}(t) \cdot f(S_{j,k+1/2}^+(t)) + y_{v_{j,k+1/2}}(t) \cdot f(S_{j,k+1/2}^-(t)) \right] \\ &\quad - \frac{a_{j,k+1/2}^y(t)}{2} \left[S_{j,k+1/2}^+(t) - S_{j,k+1/2}^-(t) \right]. \end{aligned} \quad (17b)$$

Here, $S_{j+1/2,k}^\pm(t)$ are called the intermediate values. They are an approximate solution computed over the reconstruction $\tilde{S}_{(j+1/2)+1/2,k}(x, \mathbf{y}_k, t)$ at the point $(x_{j+1/2}, y_k)$, that is,

$$S_{j+1/2,k}^+(t) := \tilde{S}_{j+1,k}(x_{j+1/2}, \mathbf{y}_k, t) = \bar{S}_{j+1,k}(t) - \frac{\Delta X}{2} (S_x)_{j+1,k}(t). \quad (18)$$

Analogously,

$$S_{j,k+1/2}^+(t) := \tilde{S}_{j,k+1}(\mathbf{x}_j, y_{k+1/2}, t) = \bar{S}_{j,k+1}(t) - \frac{\Delta Y}{2} (S_y)_{j,k+1}(t). \quad (19)$$

The numerical derivatives are computed using the MinMod limiter given by Equation (12). In our numerical experiments, the parameter θ assumes the values $1 < \theta < 1.8$. The local speeds of propagation $a_{j+1/2,k}^x(t)$ and $a_{j,k+1/2}^y(t)$ are estimated at the cell boundaries $(x_{j+1/2}, y_k)$ and $(x_j, y_{k+1/2})$, respectively, as the upper bound

$$a_{j+1/2,k}^x(t) = \max \left\{ |x_{v_{j+1/2,k}}(t) \cdot f'(S_{j+1/2,k}^+(t))|, |x_{v_{j+1/2,k}}(t) \cdot f'(S_{j+1/2,k}^-(t))| \right\} \quad (20a)$$

$$a_{j,k+1/2}^y(t) = \max \left\{ |y_{v_{j,k+1/2}}(t) \cdot f'(S_{j,k+1/2}^+(t))|, |y_{v_{j,k+1/2}}(t) \cdot f'(S_{j,k+1/2}^-(t))| \right\}, \quad (20b)$$

considering convex fluxes for simplicity.

Here the velocity field used in the KT scheme is obtained directly from Raviart-Thomas space on the cell edges:

$$\begin{aligned} {}^x v_{j+1/2,k}(t) &:= (v_r)_{jk}(t), & {}^x v_{j-1/2,k}(t) &:= (v_l)_{jk}(t), \\ {}^y v_{j,k+1/2}(t) &:= (v_u)_{jk}(t), & {}^y v_{j,k-1/2}(t) &:= (v_d)_{jk}(t); \end{aligned}$$

where v_r, v_l, v_u, v_d stand for the velocity on the “right”, “left”, “up” and “down” faces of the cells.

The two-dimensional semi-discrete formulation (16) comprises a system of nonlinear ordinary differential equations for the discrete unknowns $\{S_{j,k}(t)\}$. To solve it, we integrate in time introducing a variable time step Δt_c . Although the forward Euler scheme can be used, it may be advantageous to use higher order discretizations in numerical simulations. The numerical examples presented below use third-order Runge-Kutta ODE solvers based on convex combinations of forward Euler steps. See Shu (1988) and Shu and Osher (1988) for more details on a whole family of such schemes.

4. TWO-DIMENSIONAL NUMERICAL EXPERIMENTS

We present and compare the results for numerical simulations of two-dimensional, two-phase flow associated with two distinct flooding problems using the KT and NT schemes. We first consider two-dimensional flow in a rectangular, heterogeneous reservoir (*slab geometry*) having $256 \text{ m} \times 64 \text{ m}$ and then we discuss results of two-dimensional flow simulations in a 5-spot pattern, homogeneous reservoir. In the 5-spot geometry we used two distinct uniform five-spot well configurations intended to illustrate different flow patterns with parallel and diagonal grid orientations, and boundary behavior having $90 \text{ m} \times 90 \text{ m}$ and $64 \text{ m} \times 64 \text{ m}$, respectively, of physical dimensions.

In all simulations, the reservoir contains initially 79% of oil and 21% of water. Water is injected at a constant rate of 0.2 pore volumes every year. The fractional volumetric flow, the total mobility, and the relative permeabilities are assumed to be:

$$f(s) = \frac{k_{rw}(s)/\mu_w}{\lambda(s)}, \quad \lambda(s) = \frac{k_{rw}(s)}{\mu_w} + \frac{k_{ro}(s)}{\mu_o},$$

and

$$k_{ro}(s) = (1 - (1 - s_{ro})^{-1}s)^2, \quad k_{rw}(s) = (1 - s_{rw})^{-2}(s - s_{rw})^2,$$

where $s_{ro} = 0.15$ and $s_{rw} = 0.2$ are the residual oil and water saturations, respectively.

For the heterogeneous reservoir studies we consider a scalar absolute permeability field $K(\mathbf{x})$ taken to be log-normal (a fractal field, see (Glimm et al., 1993) and (Furtado and Pereira, 2003) for more details) with moderately large heterogeneity strength. The spatially variable permeability field is defined on 256×64 grid with three different values of the coefficient of variation CV (standard deviation)/mean: 0.5, 1.2, and 2.2. The boundary conditions and injection and production specifications for the two-phase flow equations (1)-(2) are as follows. For the horizontal slab geometry, injection is made uniformly along the left edge of the reservoir and the (total) production rate is taken to be uniform along the right edge; no flow is allowed along the edges appearing at the top and bottom of the reservoir in the graphics (Figures 2, 3, and 4).

In the case of a five-spot flood discretized by a diagonal grid (Figure 5), injection takes place at one corner and production at the diametrically opposite corner; no flow is allowed across the entirety of the boundary. In the case of a five-spot flood discretized by a parallel grid (Figure 6), injection takes place at two diametrically opposite corners (say, left down and right up), and production in the diametrically 'off diagonal' (say, right down and left up). However, to better illustrate different flow patterns with parallel and diagonal grid orientations along with the boundary behavior, the well configuration for the numerical results obtained with both parallel and diagonal grids are in agreement (see Figures 5 and 6).

We now discuss the simulations in the slab geometry. Figures 2, 3, and 4 refers to a comparison study for the NT and KT schemes, showing the water saturation surface plots after 275, 250 and 225 days of simulation for three different values for the strength of the heterogeneity of the fractal permeability field, $CV = 0.5$, 1.2 , and 2.2 . The viscosity of oil and water used in all numerical examples are $\mu_o = 10.0 \text{ cP}$ and $\mu_w = 0.05 \text{ cP}$.

The results using the NT scheme were computed with grids having 256×64 , 512×128 and 1024×256 cells (the first three pictures from top to bottom) of the Figures 2, 3, and 4. In the bottom pictures of the Figures 2, 3, and 4, we use the KT scheme on a 256×64 computational grid.

It is unquestionable that the KT scheme gives a more accurate solution than the solutions computed by the NT scheme. Also we can see in these figures that we need to refine twice the grid used in the NT scheme or, in other words, multiply by 16 the number of the cells to produce an equivalent solution given by the KT scheme using the coarsest grid. However, as the heterogeneity gets higher the solution given by the KT scheme experiences some little spurious oscillations near the shocks and at the bottom boundary of the reservoir, even under the stability conditions stated in Kurganov and Tadmor (2000) (see Figure 4).

We now turn to the discussion of the set of simulations performed in a five-spot pattern for an homogeneous reservoir. Figures 5 (diagonal grid) and 6 (parallel grid) shows the saturation level curves after 260 days of simulation obtained with the NT and KT schemes for two levels of spatial discretization.

In both Figures 5 (diagonal grid) and 6 (parallel grid), the pictures on the left column are the results obtained with the NT scheme and the ones on the right were computed with the KT scheme. In these Figures, the grids are refined from top to bottom and have 64×64 and 128×128 cells in the diagonal pattern and 90×90 and 180×180 cells in the parallel grid.

It is clear that the KT scheme (right column pictures in Figure 5; diagonal grid) is producing incorrect boundary behavior. Moreover, as the computational grid is refined (right column and bottom picture in Figure 5) this problem seems to be emphasized. However, the KT scheme in a parallel grid configuration (right column pictures in Figure 6) is not producing incorrect boundary behavior.

Although considerably less diffusive, the KT scheme may produce incorrect behaviors in both the slab and Five-Spot numerical examples. We remark that these incorrect behaviors are not present in the NT scheme. We list some factors that might be leading to these problems:

- the dimension by dimension approach is an approximation of a genuinely two dimensional problems. The KT scheme uses numerical fluxes in the x and y directions which can be viewed as generalizations of one-dimensional numerical fluxes.
- the boundary conditions and the injection and production specifications;
- the velocity field used in the KT scheme;
- or even a combination of these factors.

To investigate these problems one might study each one of the factors listed above. The authors are currently working on an improvement of these schemes in order to compute a more precise numerical flux.

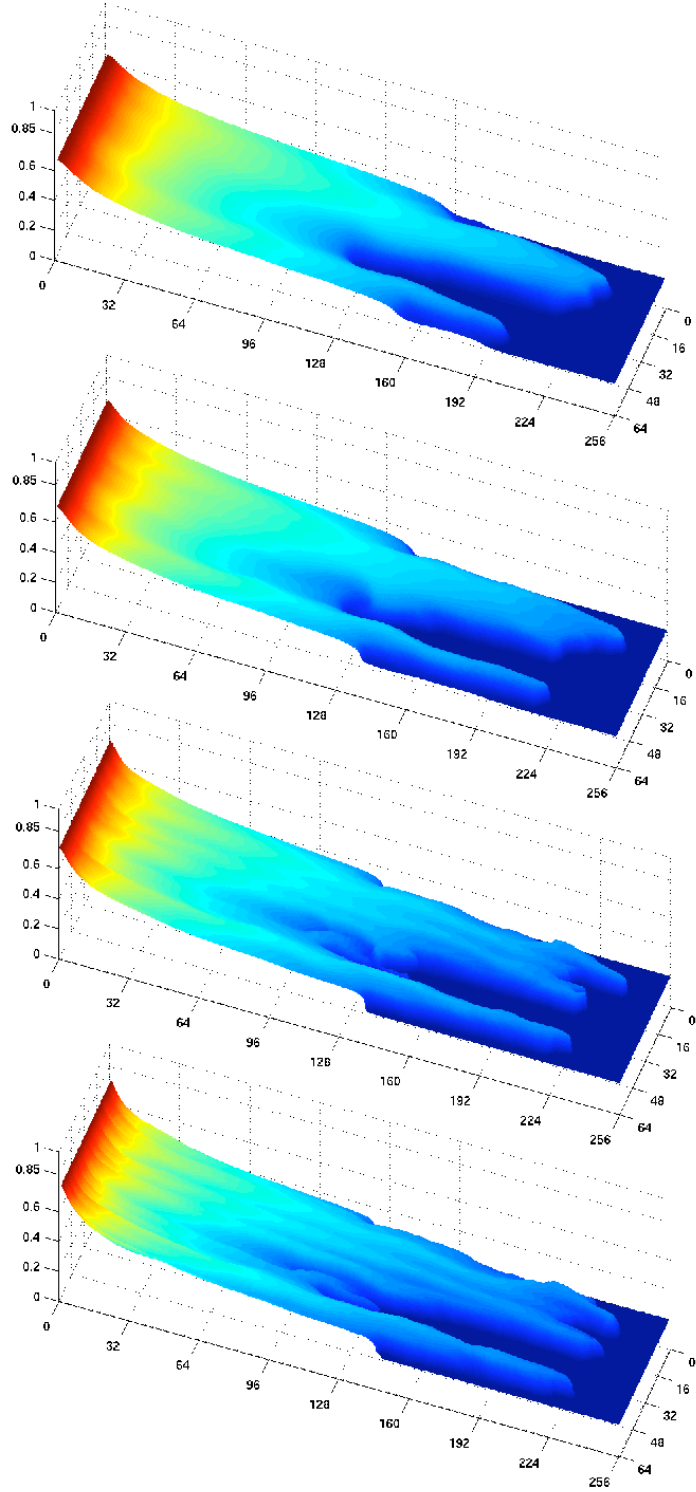


FIGURE 2. Water saturation surface plots after 275 days of simulation in a heterogeneous reservoir having $256 \text{ m} \times 64 \text{ m}$, with $CV = 0.5$ and viscosity ratio 20. The first three pictures from top to bottom used the NT scheme with grids having 256×64 , 512×128 and 1024×256 cells, respectively. The bottom picture shows the KT scheme with a grid of 256×64 cells.

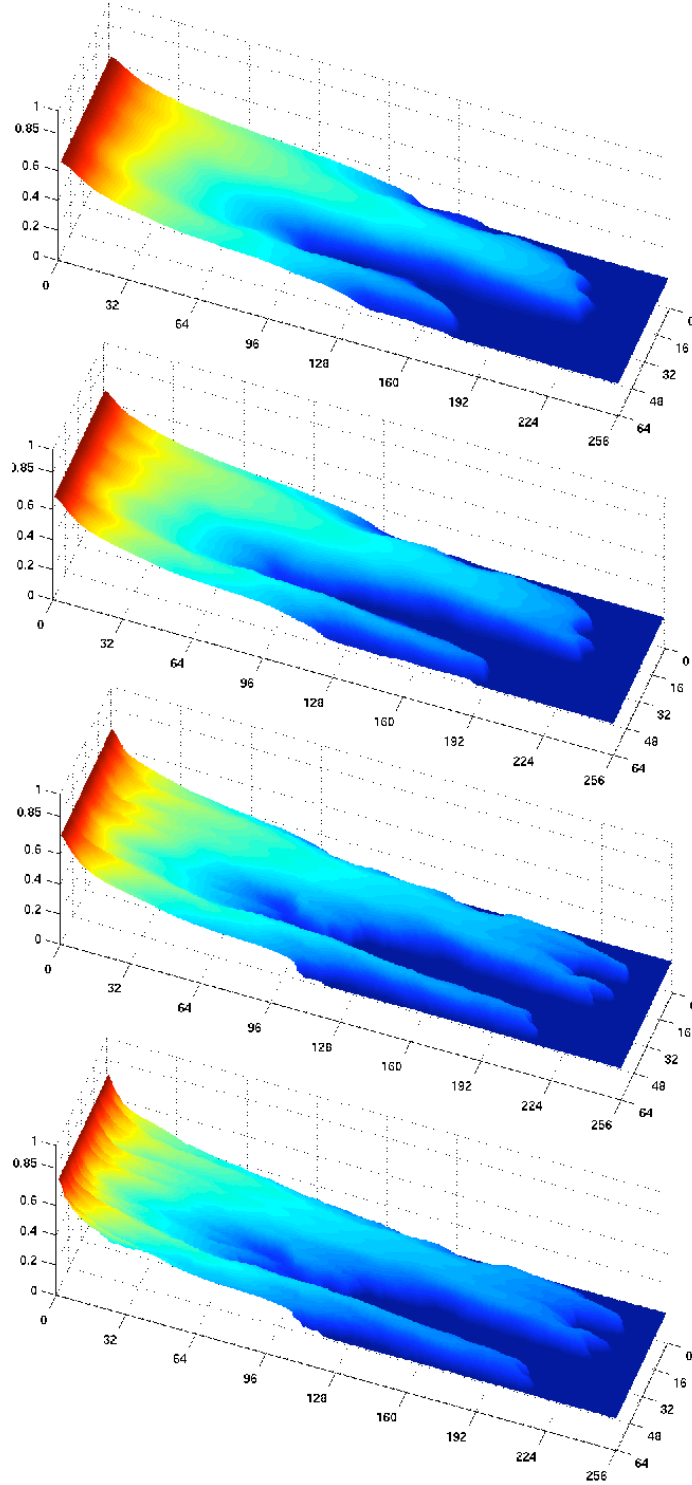


FIGURE 3. Water saturation surface plots after 250 days of simulation in a heterogeneous reservoir having $256 \text{ m} \times 64 \text{ m}$, with $CV = 1.2$ and viscosity ratio 20. The first three pictures from top to bottom used the NT scheme with grids having 256×64 , 512×128 and 1024×256 cells, respectively. The bottom picture shows the KT scheme with a grid of 256×64 cells.

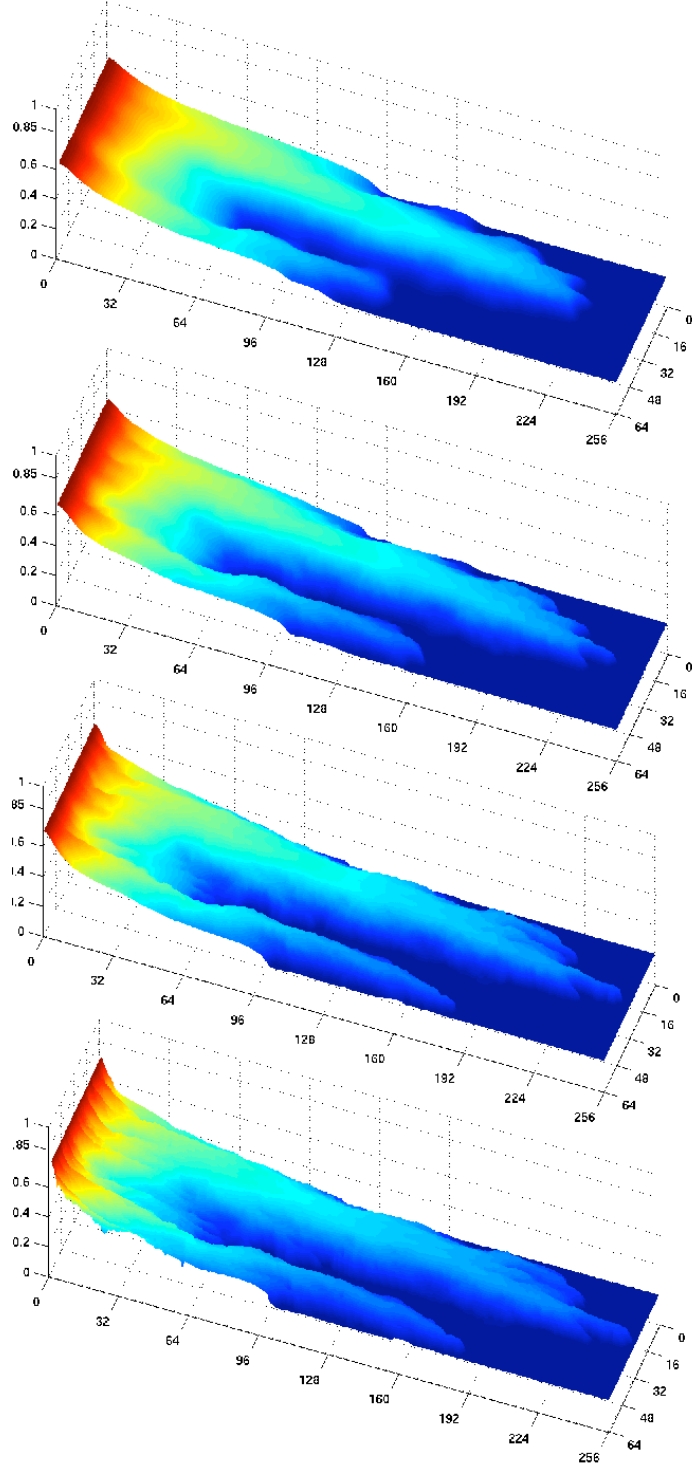


FIGURE 4. Water saturation surface plots after 225 days of simulation in a heterogeneous reservoir having $256 \text{ m} \times 64 \text{ m}$, with $CV = 2.2$ and viscosity ratio 20. The first three pictures from top to bottom used the NT scheme with grids having 256×64 , 512×128 and 1024×256 cells, respectively. The bottom picture shows the KT scheme with a grid of 256×64 cells.

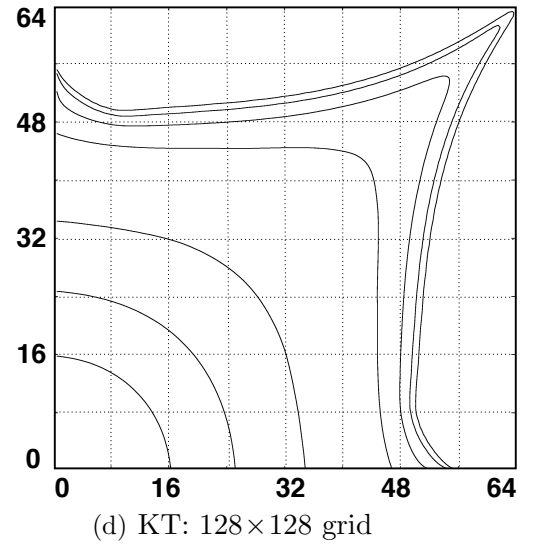
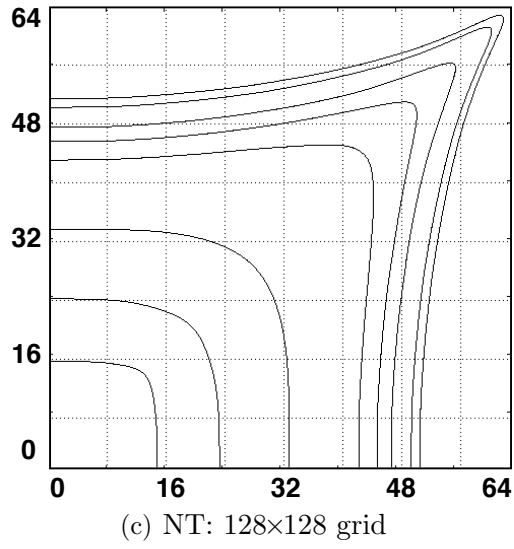
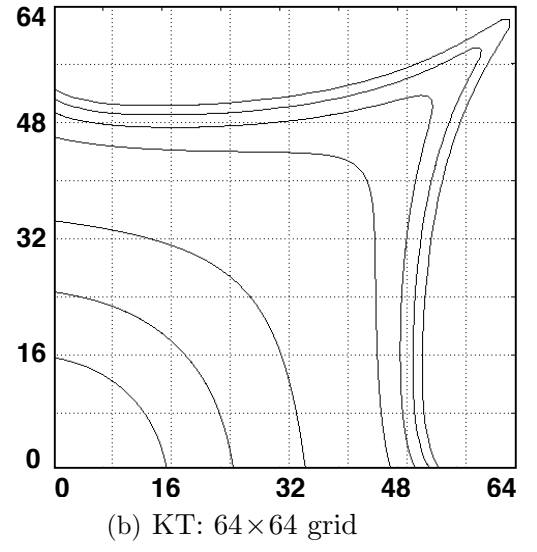
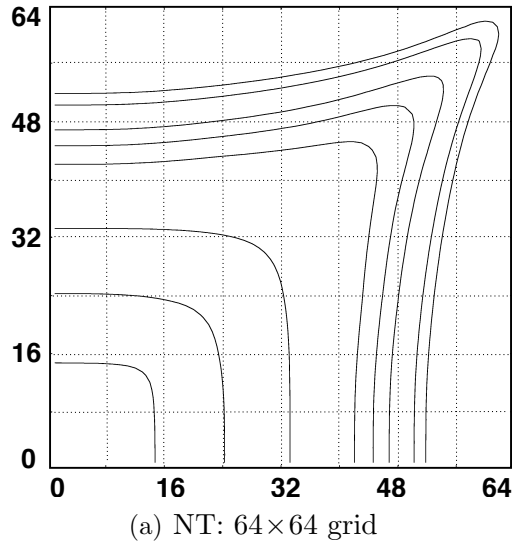


FIGURE 5. Water saturation level curves for two-phase flow in a five-spot well configuration - diagonal grid.

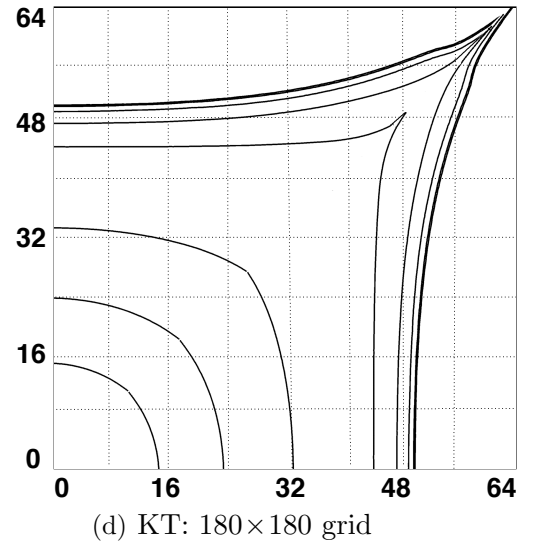
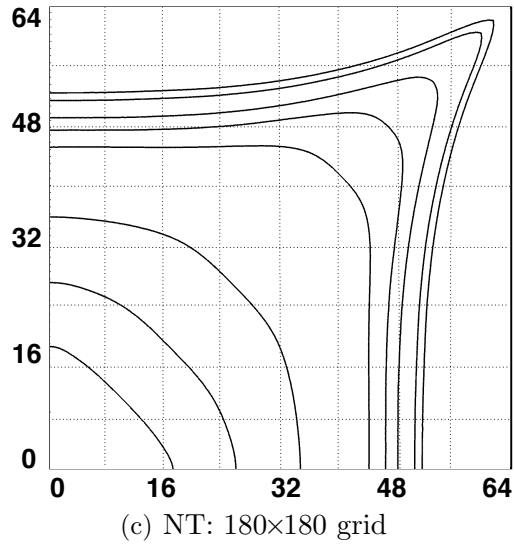
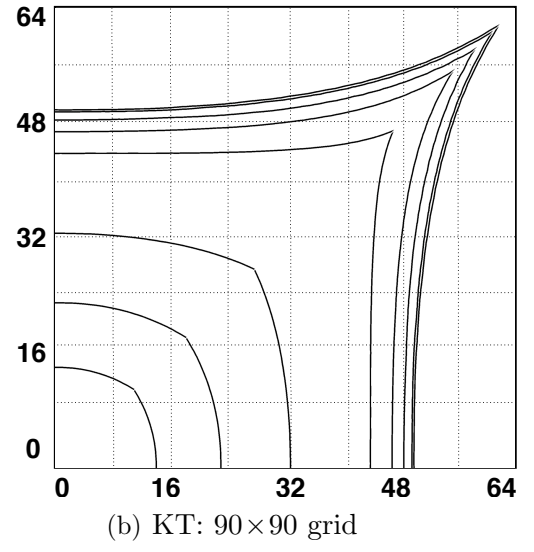
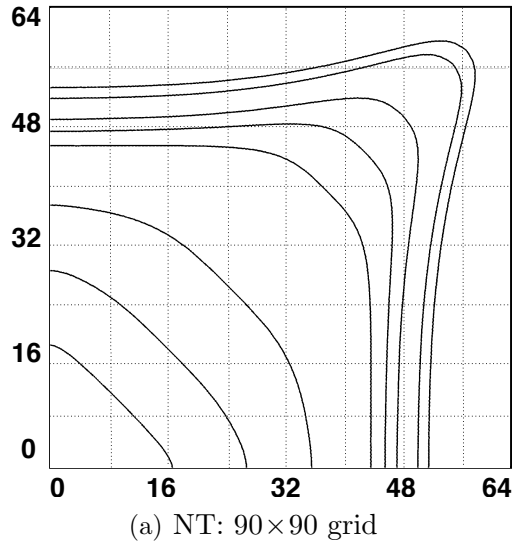


FIGURE 6. Water saturation level curves for two-phase flow in a five-spot well configuration - parallel grid.

REFERENCES

- E. Abreu, F. Furtado, D. Marchesin, and F. Pereira. Transitional waves in three-phase flows in heterogeneous formations. *Computational Methods for Water Resources*, I: 609–620, 2004a.
- E. Abreu, F. Furtado, D. Marchesin, and F. Pereira. Three-phase flow in petroleum reservoirs. *Proceedings of the Conference on Analysis, Modeling and Computation of PDEs and Multiphase Flow, in Celebration of James Glimm’s 70th Birthday, SUNY at Stony Brook*. To appear, 2004b.
- E. Abreu, F. Furtado, and F. Pereira. Three-phase immiscible displacement in heterogeneous petroleum reservoirs. To appear in the *Journal of Applied Numerical Mathematics*, 2004c.
- E. Abreu, F. Furtado, and F. Pereira. On the numerical simulation of three-phase reservoir transport problems. *Transport Theory Statist. Phys.*, 33(5-7):503–526, 2004d.
- J. B. Bell, C. N. Dawson, and G. B. Shubin. An unsplit high-order godunov scheme for scalar conservation laws in two dimensions. *J. Comput. Phys.*, 75(5-7):1–24, 1988.
- G. Chavent and J. Jaffré. *Mathematical Methods and Finite Elements for Reservoir Simulation*, volume 17. Studies in Mathematics and its Applications, North-Holland, Amsterdam, studies in mathematics and its applications edition, 1986.
- A. L. G. A. Coutinho and I. D Parsons. Finite element multigrid methods for two-phase immiscible flow in heterogeneous media. *Communications in Numerical Methods in Engineering*, 15:1–7, 1999.
- A.L.G.A. Coutinho, J.L.D. Alves, E.L.M. Garcia, and A.F.D. Loula. Solution of miscible and immiscible flows employing element-by-element iterative strategies. *3rd SPE Latin American/Caribbean Engin.Conference*, pages 431–444, 1994.
- H. K. Dahle, M. S. Espedal, R. E. Ewing, and O. Sævareid. Characteristic adaptive subdomain methods for reservoir flow problems. *Numer. Methods Partial Differential Equations*, 6(4):279–309, 1990.
- H. K. Dahle, R. E. Ewing, and T. F. Russell. Eulerian-Lagrangian localized adjoint methods for a nonlinear advection-diffusion equation. *Comput. Methods Appl. Mech. Engrg.*, 122(3-4):223–250, 1995.
- J. Douglas, Jr., F. Furtado, and F. Pereira. On the numerical simulation of waterflooding of heterogeneous petroleum reservoirs. *Comput. Geosci.*, 1(2):155–190, 1997.
- J. Douglas, Jr., F. Pereira, and Li-Ming Yeh. A locally conservative Eulerian-Lagrangian method for flow in a porous medium of a mixture of two components having different densities. In *Numerical treatment of multiphase flows in porous media (Beijing, 1999)*, volume 552 of *Lecture Notes in Phys.*, pages 138–155. Springer, Berlin, 2000.
- Jim Douglas, Jr. and Thomas F. Russell. Numerical methods for convection-dominated diffusion problems based on combining the method of characteristics with finite element or finite difference procedures. *SIAM J. Numer. Anal.*, 19(5):871–885, 1982.
- L.J. Durlofsky. A triangle based mixed finite element-finite volume technique for modeling two phase flow through porous media. *Journal of Computational Physics*, 105:252–266, 1993.
- R. E. Ewing and H. Wang. A summary of numerical methods for time-dependent advection-dominated partial differential equations. *J. Comput. Appl. Math.*, 128(1-2):

- 423–445, 2001. Numerical analysis 2000, Vol. VII, Partial differential equations.
- F. Furtado and F. Pereira. Crossover from nonlinearity controlled to heterogeneity controlled mixing in two-phase porous media flows. *Comput. Geosci.*, 7(2):115–135, 2003.
- J. Glimm, B. Lindquist, O. McBryan, and L. Padmanabhan. A front tracking reservoir simulator: 5-spot validation studies and the water coning problem. *Frontiers in Applied Mathematics*, H. T. Banks, 1, 1983.
- J. Glimm, B. Lindquist, F. Pereira, and Q. Zhang. A theory of macrodispersion for the scale up problem. *Transport in Porous Media*, 13:97–122, 1993.
- S. K. Godunov. A difference method for numerical calculation of discontinuous solutions of the equations of hydrodynamics. *Mat. Sb. (N.S.)*, 47 (89):271–306, 1959.
- A. Kurganov and E. Tadmor. New high-resolution central schemes for nonlinear conservation laws and convection-diffusion equations. *J. Comput. Phys.*, 160(1):241–282, 2000.
- P.D. Lax. Weak solutions of non-linear hyperbolic equations and their numerical computation. *Comm. Pure Appl. Math.*, 7:159–193, 1954.
- H. Nessyahu and E. Tadmor. Nonoscillatory central differencing for hyperbolic conservation laws. *J. Comput. Phys.*, 87(2):408–463, 1990.
- D. W. Peaceman. *Fundamentals of Numerical Reservoir Simulation*. Elsevier, New York, 1977.
- P.-A. Raviart and J. M. Thomas. A mixed finite element method for 2nd order elliptic problems. In *Mathematical aspects of finite element methods (Proc. Conf., Consiglio Naz. delle Ricerche (C.N.R.), Rome, 1975)*, pages 292–315. Lecture Notes in Math., Vol. 606. Springer, Berlin, 1977.
- V. V. Rusanov. The calculation of the interaction of non-stationary shock waves with barriers. *Ž. Vyčisl. Mat. i Mat. Fiz.*, 1:267–279, 1961.
- C. W. Shu. Total variation diminishing time discretizations. *SISSC*, 6:1073, 1988.
- C. W. Shu and S. Osher. Efficient implementation of essentially non-oscillatory shock capturing schemes. *Journal of Computational Physics*, 77:439, 1988.
- B. Van Leer. Towards the ultimate conservative difference scheme. v. a second order sequel to godunov’s method. *J. Comp. Phys.*, 32:101–136, 1979.